

AD-A247 011



PL-TR-91-2126

E 100 100

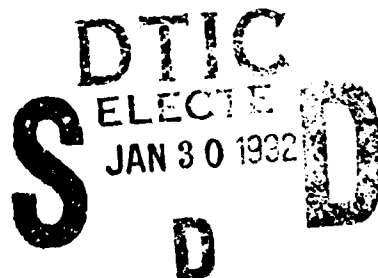
2

**STUDIES OF REGIONAL WAVE PROPAGATION USING DIFFERENTIAL
SEISMOGRAMS AND RANDOMIZED STRUCTURAL MODELS**

Danny J. Harvey

University of Colorado/CIRES
Campus Box 449
Boulder, CO 80309

7 May 1991



Final Report
1 March 1990 - 1 March 1991

Approved for public release; distribution unlimited



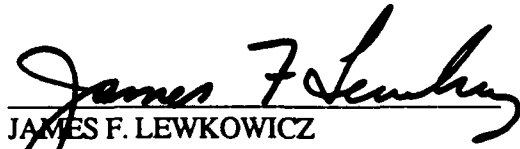
**PHILLIPS LABORATORY
AIR FORCE SYSTEMS COMMAND
HANSCOM AIR FORCE BASE, MASSACHUSETTS 01731-5000**


92-02341



The views and conclusions contained in the document are those of the authors and should not be interpreted as representing the official policies, either expressed or implied, of the Air Force or the U.S. Government.

This technical report has been reviewed and is approved for publication.


JAMES F. LEWKOWICZ
Contract Manager
Solid Earth Geophysics Branch
Earth Sciences Division


JAMES F. LEWKOWICZ
Branch Chief
Solid Earth Geophysics Branch
Earth Sciences Division


DONALD H. ECKHARDT, Director
Earth Sciences Division

This document has been reviewed by the ESD Public Affairs Office (PA) and is releasable to the National Technical Information Service (NTIS).

Qualified requestors may obtain additional copies from the Defense Technical Information Center. All others should apply to the National Technical Information Service.

If your address has changed, or if you wish to be removed from the mailing list, or if the addressee is no longer employed by your organization, please notify PL/IMA, Hanscom AFB MA 01731-5000. This will assist us in maintaining a current mailing list.

Do not return copies of this report unless contractual obligations or notices on a specific document requires that it be returned.

REPORT DOCUMENTATION PAGE			Form Approved OMB No 0704-0188	
1. AGENCY USE ONLY (Leave blank)		2. REPORT DATE May 7, 1991	3. REPORT TYPE AND DATES COVERED Final 1 March 1990 - 1 March 1991	
4. TITLE AND SUBTITLE Studies of Regional Wave Propagation Using Differential Seismograms and Randomized Structural Models			5. FUNDING NUMBERS C F19628-90-K-0023 PE 61102F PR 7600 TA09 WUAM	
6. AUTHOR(S) Danny J. Harvey				
7. PERFORMING ORGANIZATION NAME(S) AND ADDRESS(ES) The University of Colorado/CIRES Campus Box 449 Boulder, CO 80309			8. PERFORMING ORGANIZATION REPORT NUMBER	
9. SPONSORING MONITORING AGENCY NAME(S) AND ADDRESS(ES) Phillips Laboratory Hanscom AFB, MA 01721-5000 Contract Manager: James Lewkowicz/LWH			10. SPONSORING MONITORING AGENCY REPORT NUMBER PL-TR-91-2126	
11. SUPPLEMENTARY NOTES				
12a. DISTRIBUTION/AVAILABILITY STATEMENT approved for public release; distribution unlimited			12b. DISTRIBUTION CODE	
13. ABSTRACT (Maximum 200 words) In order to improve our abilities to discriminate low-yield nuclear explosions and to obtain accurate yield estimates, a study has been undertaken to infer detailed source and structural parameters by direct inversion of broad band seismic data using laterally homogeneous forward modeling methods. Three key problems have been identified which must be solved: the development of an accurate and efficient algorithm for computing differential seismograms, which are necessary for the inversion procedure, the development of better methods for incorporating anelastic attenuation into modal synthesis computations, and the determination of starting solutions that will produce synthetic seismograms which have the same general characteristics that we see in the data. An exact differential seismogram algorithm has been developed and implemented which produces accurate differential seismograms at arbitrary frequencies and phase velocities. An exact complex pole based algorithm has been developed to account for anelastic attenuation. A new representation of earth upper mantle and crustal structure has been used which provides an explainable, plausible and implementable method for modeling the features that we see in regional broad band data.				
14. SUBJECT TERMS Regional Wave Propagation, Differential Seismograms, Seismic Scattering			15. NUMBER OF PAGES 38	
			16. PRICE CODE	
17. SECURITY CLASSIFICATION OF REPORT UNCLASSIFIED	18. SECURITY CLASSIFICATION OF THIS PAGE UNCLASSIFIED	19. SECURITY CLASSIFICATION OF ABSTRACT UNCLASSIFIED	20. LIMITATION OF ABSTRACT UL	

Studies of Regional Wave Propagation Using Differential Seismograms and Randomized Structural Models

by

Danny J. Harvey



Accession For	
NTIS	CRAQI
DTIC	TAB
U. S. Government	
Justification	
Ey	
Distribution	
Availability Codes	
Dist	Availability Codes
A-1	

1. Introduction

In order to significantly improve the ability to detect underground nuclear explosions using seismic measurements and to minimize the biases and uncertainties associated with yield estimations, there has been a recent trend towards the use of extended-band seismic data in regional distance ranges. This data holds out the potential of higher resolving power than the traditional teleseismic data which has been used over the years for monitoring underground nuclear testing in the Soviet Union, however the regional discriminants in use today have been determined largely in an empirical fashion from data collected in the United States and their applicability to other regions, such as the Soviet Union, is not completely obvious. This is due to the fact that we do not understand, from a theoretical seismological standpoint, many of the properties of seismic arrivals that are used in regional discriminants, P_n , S_n , P_p and L_p , thus making it difficult to extrapolate these properties to a different setting.

Confidence in our discrimination and yield estimation methods is, to a large extent, dependent upon our understanding of P_n , S_n , P_p and L_p propagation and the roles played by frequency dependent anelastic attenuation and the depth dependence of structural elastic parameters in the crust, at the Moho and in the upper mantle. Suitable velocity gradients in the vicinity of a major structural discontinuity, such as the Moho, can have large effects on the associated seismic arrival, P_n , and low velocity zones or zones of "randomized laminations" within the crust can act as very efficient waveguides to trap seismic

arrivals, such as P_n . Simple ray-based modeling, that has been very successful at teleseismic distances, can produce incorrect and misleading results when applied to regional problems. In addition, we have found that even "complete" synthesis methods can mislead us if we fail to represent the fundamental characteristics of hypothetical structural models correctly.

In this paper we report on the initial results of a long term study which is aimed at obtaining understanding of the fundamental processes involved in regional seismic wave propagation and what the data that we observe tell us about the nature of the earth's crust and upper mantle. With this knowledge we will be able to more confidently resolve detailed source characteristics and make it possible to significantly improve detection and yield estimation capabilities.

Our basic objective is to develop an inversion algorithm which will directly compare broadband regional data with complete synthetic seismograms to infer detailed structure and source properties. This objective is ambitious and touches on most areas of seismology, both observational and theoretical. As a starting point, we began by using the results of other researchers, such as Gombert and Masters,¹ who have successfully inverted for crust and upper mantle structural parameters by directly comparing complete locked mode synthetic seismograms with the observed data in the time domain. The key to this inversion is the use of synthetic differential seismograms which describe the linearized relationship between model parameters and the resulting synthetic seismograms. These provide the Frechet derivatives that are necessary in the inversion and it is important that they be computed accurately and efficiently.

Previous inversion efforts of this type have all been limited to low frequencies (less than 0.2 Hz) and have directly compared synthetics with data in the time domain. Our

¹ Gombert, J. and Masters, T., 1988, Waveform modelling using locked-mode synthetic and differential seismograms: application to determination of the structure of Mexico, *Geophysical Journal of the Royal Astronomical Society*, V. 94, p. 193-218.

objective is to push this inversion to the highest frequencies that will produce useful results and we would certainly hope to get to at least 1 Hz. In order to accomplish this it is necessary to solve the following key problems.

- The development of an accurate and efficient algorithm for computing differential seismograms which are necessary for the inversion procedure.
- The development of better methods for incorporating anelastic attenuation into modal synthesis computations.
- The determination of starting solutions that will produce synthetic seismograms which have the same general characteristics that we see in the data.

In section 2 we discuss our results in developing an exact differential seismogram program. This was necessary because the traditional first order perturbation method for computing differential seismograms proved to be inadequate for our problem. In section 3 we talk about how we have dealt with the problems related with anelastic attenuation and in section 4 we show results that give us a powerful new way of looking at the earth's crust which provides us with an easy method for modeling many of the characteristics that we see in broad band regional data.

2. Computation of Differential Seismograms at High Frequencies

The standard method for computing differential seismograms makes use of first order perturbation (FOP) theory and is described by Takeuchi and Saito.² In this technique Rayleigh's principle is used to find expressions for the effects of small changes of the elastic properties on the phase velocities of normal modes. These expressions relate the partial derivatives of the eigenvalues to depth integrals of the un-perturbed eigenfunctions and make it possible to compute eigenvalue derivatives implicitly without direct application of the chain rule through the entire sequence of computations. The

² Takeuchi, H. and Saito, M., 1972, Seismic Surface Waves. Methods in Computational Physics, v. 11, p. 217-294, ed. Bolt, B., Academic Press, New York

resulting formalism makes it possible to compute eigenvalue derivatives efficiently and accurately and this method has been used extensively throughout the seismological community. However, the variational principle does not produce eigenfunction derivatives so use of this method implies that the eigenfunction derivatives will be neglected in the final differential seismograms.

In cylindrical coordinates we can express the frequency dependent P-SV displacement vector, \mathbf{u}_n , for a single normal mode, n , as follows.

$$\mathbf{u}_n(r_r, \theta_r, z_r) = k_n \sum_m \left[[\Sigma(k_n, m)] [E(n, z_s)] \left\{ E_1(n, z_r) \hat{\mathbf{P}}(k_n, m, r_r, \theta_r) + E_2(n, z_r) \hat{\mathbf{B}}(k_n, m, r_r, \theta_r) \right\} \right] \quad (2.1)$$

where,

m is the azimuthal order number,

r_r is the radial distance to the receiver,

θ_r is the azimuth to the receiver,

z_r is the depth of the receiver,

z_s is the depth of the source,

k_n is the frequency dependent eigenwavenumber for mode n ,

$[\Sigma]$ is the frequency dependent four component source jump vector,

$[E]$ is the frequency and depth dependent four component eigenfunction vector,

$\hat{\mathbf{P}}, \hat{\mathbf{B}}$ are the \mathbf{P} and \mathbf{B} vector cylindrical harmonic components.

By simple application of the chain rule we can express a differential displacement, $\partial \mathbf{u}_n / \partial v$, where v is a model parameter, as follows.

$$\begin{aligned} \partial \mathbf{u}_n / \partial v = (\partial k_n / \partial v) \left\{ \mathbf{u}_n / k_n + k_n \sum_m \left[(\partial [\Sigma] / \partial k_n) [E] \left\{ E_1 \mathbf{P} + E_2 \mathbf{B} \right\} + [\Sigma] [E] \left\{ E_1 (\partial \mathbf{P} / \partial k_n) + E_2 (\partial \mathbf{B} / \partial k_n) \right\} \right] \right\} \\ + k_n \sum_m \left[[\Sigma] (\partial [E] / \partial v) \left\{ E_1 \mathbf{P} + E_2 \mathbf{B} \right\} + [\Sigma] [E] \left\{ (\partial E_1 / \partial v) \mathbf{P} + (\partial E_2 / \partial v) \mathbf{B} \right\} \right] \end{aligned} \quad (2.2)$$

When using FOP theory to compute differential seismograms, only the first term in equation (2.2) which depends on the eigenvalue derivative, $(\partial k_n / \partial v)$, is used and the remaining terms in (2.2) which depend on the eigenfunction derivatives, $(\partial [E] / \partial v)$, $(\partial E_1 / \partial v)$ and

$(\partial E/\partial v)$, are ignored.

Our initial implementation of a differential seismogram synthesis program used the standard FOP approach. Since we were planning on using the differential seismograms at relatively high frequencies, we felt that it would be prudent to carefully check the validity of the approximation that we were using. We did this by computing a set of difference seismograms where we took an initial structural model and computed locked mode seismograms, made a small change in a single model parameter and computed new locked mode synthetic seismograms, differenced the new seismograms with the original seismograms and repeated this process for the other model parameters. In this way we were able to obtain approximations to the exact first order Taylor series terms which included all terms in equation (2.2) and which were numerically accurate as long as the parameter changes were small enough so that the first order term in the Taylor series dominated the higher order terms.

Figure 1 shows the results of a comparison of analytic differential seismograms, labeled H4P05, which neglected the eigenfunction derivatives, versus difference seismograms, labeled S4P05. These seismograms were computed for a simple layer over a half space structure representing a crustal layer over the upper mantle and the difference and differential seismograms are with respect to the P-wave velocity in the crust layer. The bandwidth of these seismograms is 0-2 hz and the source receiver distance is 500 km. From this figure it is obvious that the analytical differential seismogram using FOP theory is in error. The time window shown in figure 1 represents the early part of the P₁ wave train and when we looked at S-wave differentials later during the Rayleigh wave we got good agreement. This shows that FOP theory is not adequate for computing differential seismograms at frequencies around 1 hz.

In order to convince ourselves that the problem was associated with neglecting the eigenfunction derivatives, we conducted an experiment where we replaced the eigenfunctions for the perturbed seismograms before differencing with those of the unperturbed

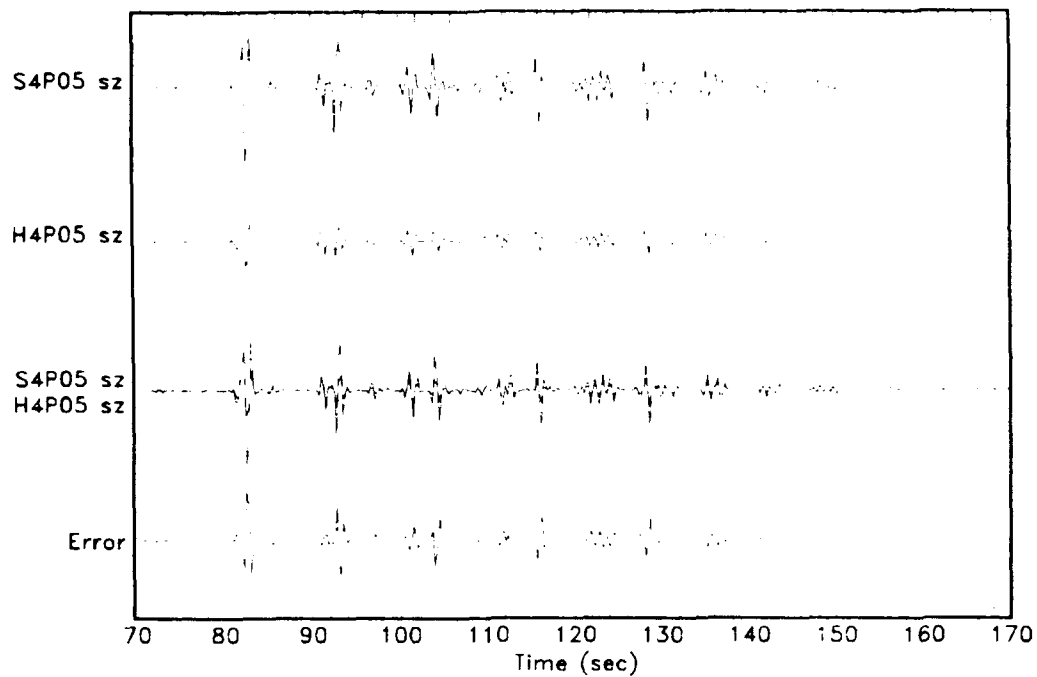


Figure 1. Difference (S4P05) vs. differential (H4P05) seismograms: eigenvalues only.

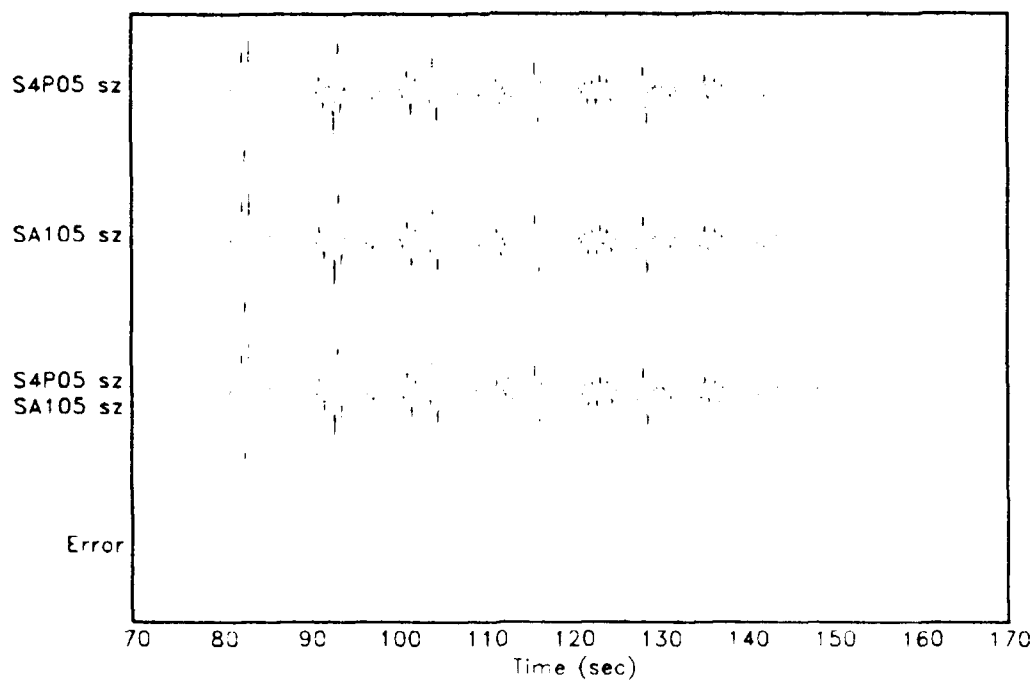


Figure 2. Difference (S4P05) vs. differential (SA105) seismograms: eigenvalues and eigenfunctions.

seismograms and recomputed difference seismograms where the eigenfunctions were forced to remain constant. In this case comparisons of our modified difference seismograms and the analytical FOP differential seismograms were very good, indicating that the problem was associated with changes in the eigenfunctions.

We then developed a computer code which computes differential seismograms analytically without neglecting the eigenfunction derivatives. This proved to be a tedious and difficult task, however we were able to develop a program which is accurate and relatively efficient, certainly when compared to the differencing approach. Our method in developing this program was straightforward:

- We abandoned using a variational principle, which involves depth integrals of the eigenfunctions, for computing the eigenvalue derivatives and replaced this approach with explicit derivative computations using the chain rule. This was a tedious and laborious process which involved carrying derivative computations through the entire chain of algebraic operations, however we found that, after some rearrangement and algebraic simplification, the resulting numerical algorithm was relatively efficient.
- We then checked that the eigenvalue derivatives matched those from the variational computations and we also checked against numerical eigenvalue derivatives from our difference seismograms.
- Since the derivative computations had been carried through all of the intermediate steps, it was then relatively straightforward to extend these computations to produce eigenfunction derivatives.
- The modal summation expressions were then modified to conform with equation (2.2) to produce exact differential seismograms.

Figure 2 shows a comparison of our exact differential seismogram, labeled SA105, with the difference seismograms, labeled S2P05. It is obvious from this figure that the comparison is very good and it is likely that the residual error is due to the numerical

approximation implicit in the difference seismogram. An example showing exact differential seismograms for a realistic regional situation with a complex structural model can be seen in figures 3 - 6. The structural P and S velocities are shown in figure 3 for a 70 layer model. As can be seen, the velocity vs. depth profiles have a random component which we will discuss in detail in section 4. This structure represents a starting estimate for the region around the Soviet nuclear test site at Semipalatinsk, KSSR. Figure 4 shows differential seismograms with respect to P-wave velocities for each layer in the model. The 70 differential seismograms are plotted one above the other as a function of layer index and the original synthetic seismogram is also shown at the top of the figure for reference. Figure 5 is the same as figure 4 except that the S-wave differential seismograms are shown. Figure 6 is a repeat of figure 4 except the vertical axis is layer index instead of depth (for comparison with figures 3 and 4).

Figures 3 and 4 give us much information about the nature of the regional seismic wave propagation for this example. The source-receiver distance is 254 km and we can see how different regions within the crust effect the resulting seismograms. The L_w coda is primarily controlled by the very near surface part of the crust although the initial portion of the arrival responds to the entire crust. The P_r coda is also strongly effected by near surface structure and we can clearly see the strong direct Moho reflection, P_nP , as a vertical streak down to layer number 55. Both P_n and S_n can also be seen in the differential seismograms at the bottom of the model.

3. Incorporation of Anelastic Attenuation in Locked Mode Synthetic Seismograms

The standard method for incorporating anelastic attenuation in modal summation seismogram synthesis methods has always involved the use of FOP theory. As we have seen with the differential seismograms, there is reason to question the accuracy of FOP theory in accounting for Q effects. Other researchers have encountered this problem³

³ Day, S., McLaughlin, K., Shkoller, B. and Stevens, J., 1989, Potential errors in locked mode synthetics for anelastic earth models, Geophysical Research Letters, v. 16, p. 203-206

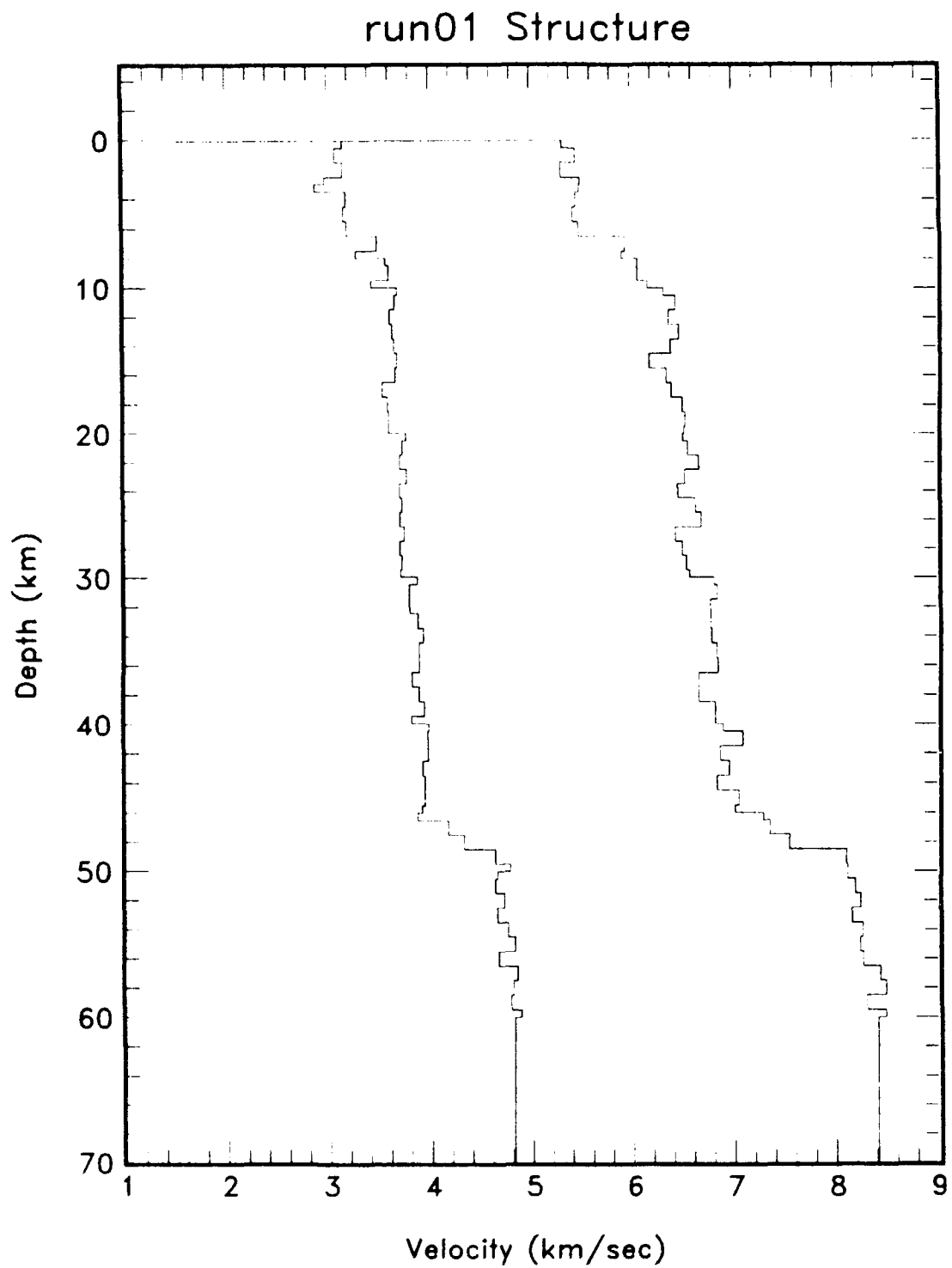


Figure 3. 70 layer randomized Kazakh structural model

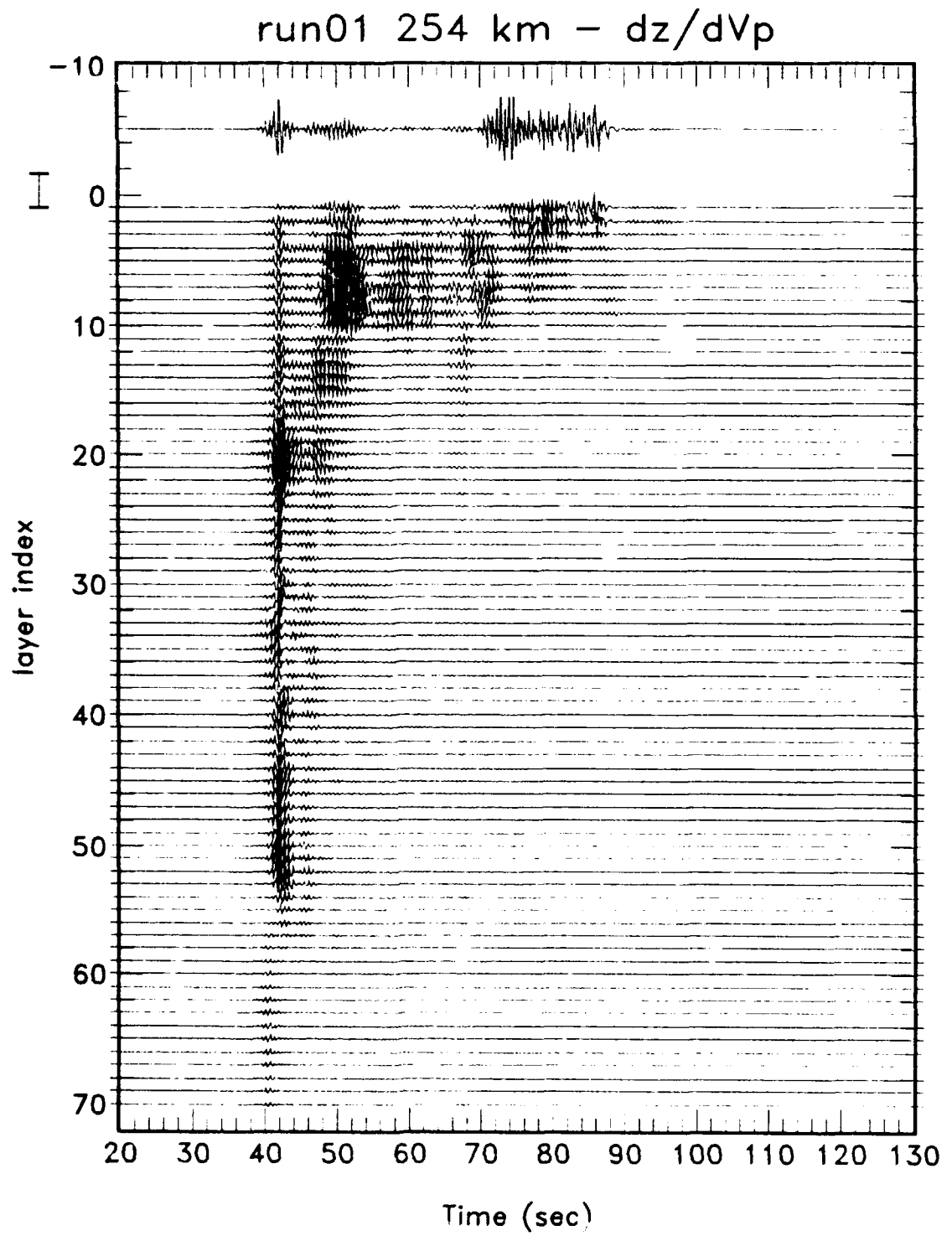


Figure 4. Differential seismograms (dz/dV_p) for the structure in fig.3.

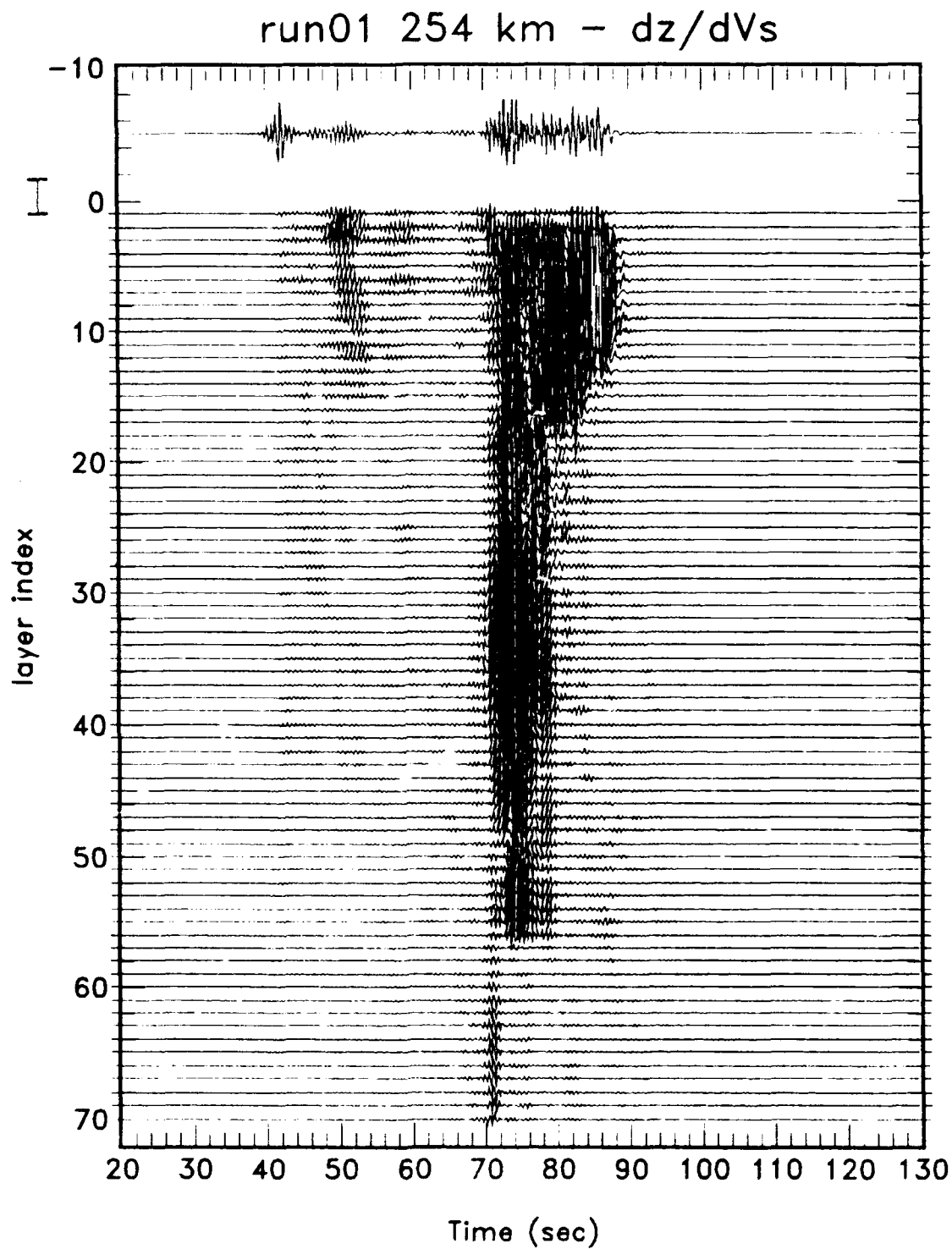


Figure 5. Differential seismograms (dz/dVs) for the structure in fig.3.

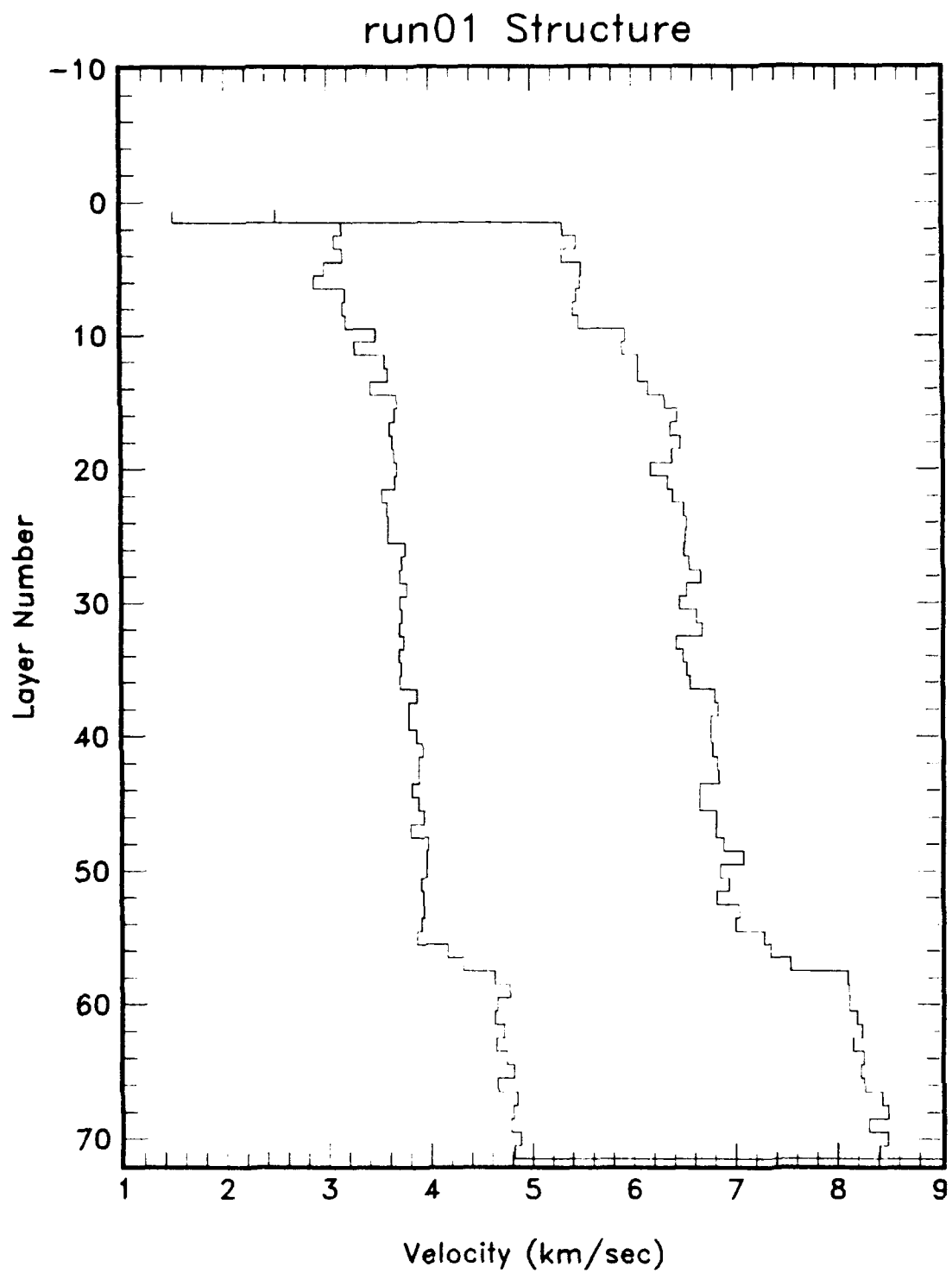


Figure 6. Structure from fig. 3 vs. layer number.

and, as with the differential seismograms, the problem seems to become more pronounced at higher frequencies and higher phase velocities.

In our early efforts to address this problem, before we had solved the differential seismogram problem, we developed a method for locating the complex eigenvalues exactly along with a complex version of the eigenfunction and modal summation codes. These programs work very well, even in situations where the Q is low, although the versions of the programs that we initially developed are not very efficient. Our success with the differential seismograms provides another track for solving the modal Q problem.

Q corrections using FOP theory involve the computation of eigenvalue shifts resulting from complex elastic parameter shifts due to the intrinsic attenuation. This normally results in purely imaginary shifts of the eigenwavenumbers⁴ which are then represented in the modal summation as frequency dependent decaying exponential terms. Thus normal modal Q corrections ignore the eigenfunction shifts in the same manner as FOP differential seismograms. In high frequency - high phase velocity situations, the resulting Q corrections are in error even for very high Q values.

We have started the development of an "exact first order" modal Q correction algorithm based upon the eigenfunction derivative capabilities that we developed for the differential seismograms. This will provide an efficient means for computing modal Q corrections that will always be accurate, as long as the Q values are sufficiently high so that the first order expansion is valid. Initial results from this work indicate that we are close to achieving this goal.

4. Velocity Randomization and Its Effects on Regional Synthetic Seismograms

When investigating an extended band regional seismogram, one is struck by the large amount of information that seems to be contained within the seismic signal. One

⁴ The shifts are purely imaginary as long as Q related dispersion effects in the real parts of the elastic wave velocities are neglected

does not see simple ray arrivals with well defined coherent wavelets, but instead, arrivals characterized by complex wavetrains with onset times that are often difficult to determine. Typical regional seismograms that were recorded near the Soviet nuclear test site at Semipalatinsk are shown in figures 7 and 8. Figure 7 shows vertical components at four stations from the Soviet JVE nuclear test as a function of receiver range from the shot site. These are all broad band seismograms (1 - 50 Hz). The stations at 170 km and 253 km were the temporarily re-occupied NRDC sites of Karasu (KSU) and Karkaralinsk (KKL) and the stations at 1350 km and 1529 km were the IRIS stations at Chusal (CHS) and Arti (ARU). Figure 8 was taken from an American Geophysical Union poster session⁵ and shows the CHS and ARU data after applying a 0.8 - 2 Hz passband filter, as well as additional data from a Peaceful Nuclear Explosion (PNE) which took place in northwestern USSR.

These data are typical of regional explosion events in the shield region of central and northern Asia and from these data we can make the following observations.

- The P_n arrival is energetic and well developed at all distances above 250 km where it first emerges from the P_r wavetrain.
- L_r is clearly defined for distances less than 2000 km but disappears above 2500 km. The L_r to P_n amplitudes stay about one.
- Apparent Q values are relatively high. High frequency energy propagates efficiently.

Most researchers attribute the incoherence of regional wavetrains to "lateral scattering" which is normally intended to mean some three dimensional distribution of structural inhomogeneities. If we assume a simple uniform distribution of scatterers in space, at a variety of wavelengths, then the scattering of a coherent wavefront propagating

⁵ Given, H., Hedlin, M., Berger, J., Vernon, F., Kappus, M., Chavez, D., and Aster, R., Regional seismic observations of nuclear explosions inside the Soviet Union, Poster presented at the American Geophysical Union meeting, December 1988, abstract appeared in EOS, Trans. Amer. Geophys. Union, v. 69, p. 1321.

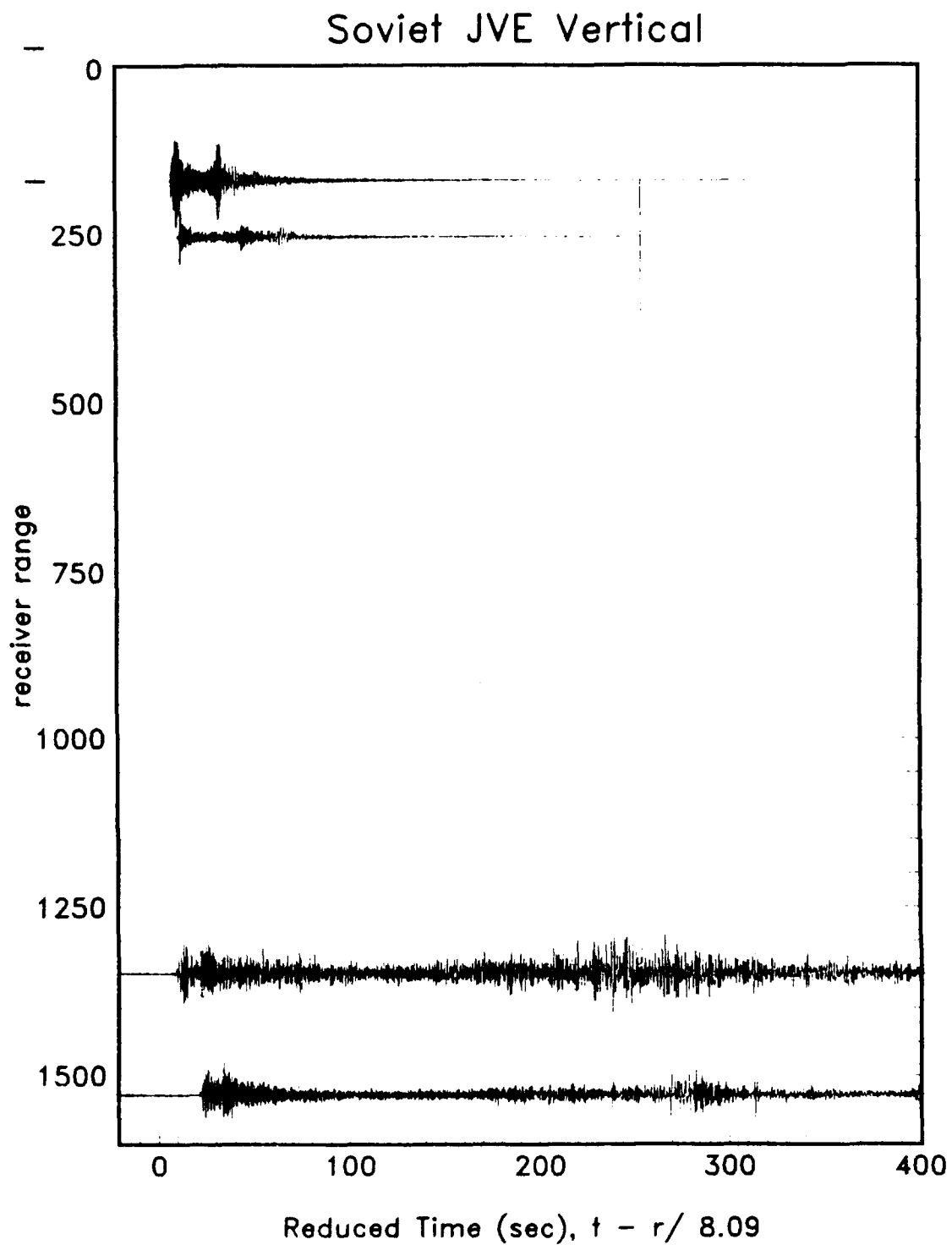


Figure 7. Vertical components recorded from the Soviet JVE nuclear test.

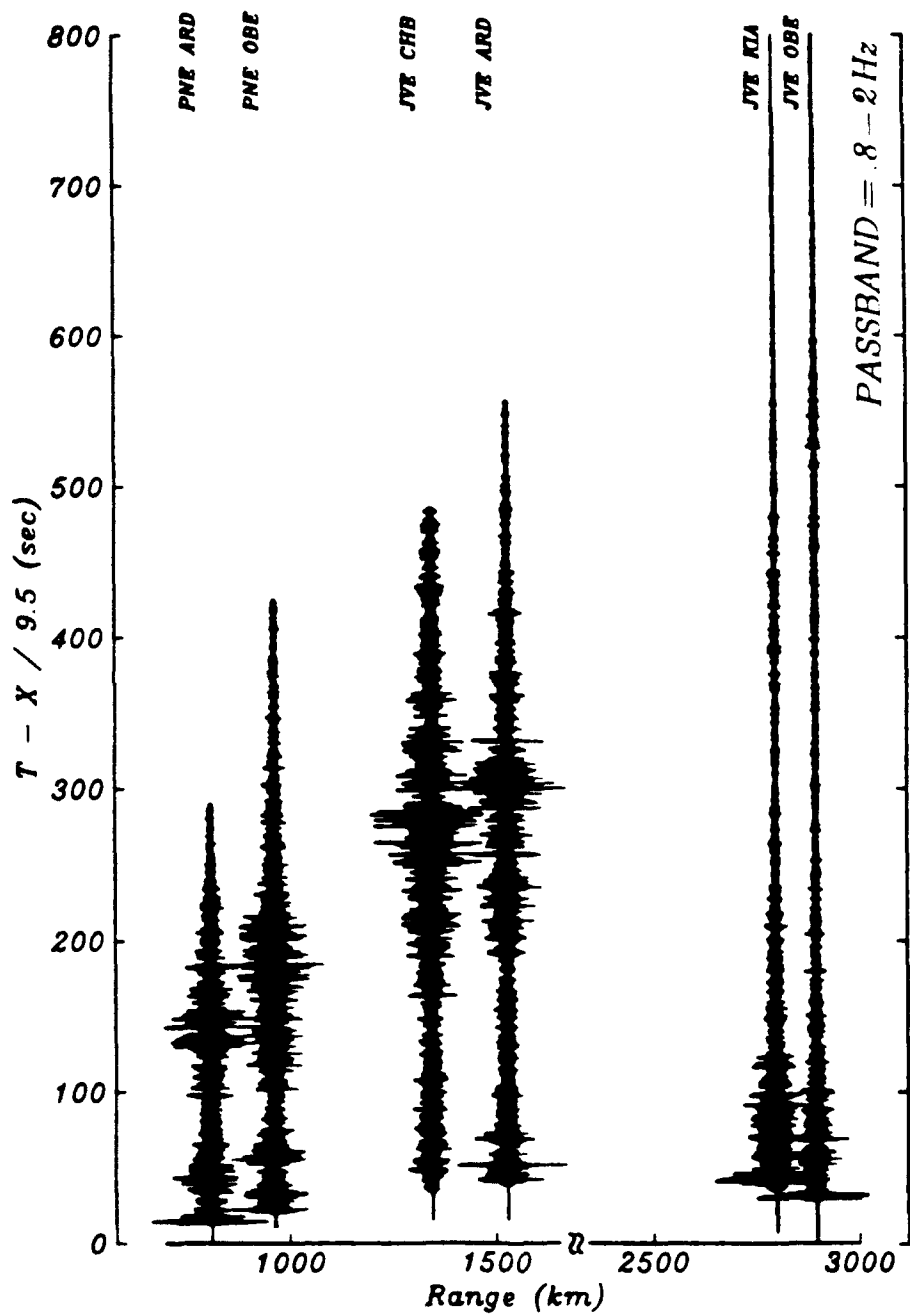


Figure 8. Seismograms from Soviet JVE and PNE, from Given, et. al.

through the medium will result in an attenuation effect of the coherent wavefront along with incoherent scattered energy that follows the coherent wavefront in a coda. The net effect is that the energy gets "smeared out" spatially so that arrivals are weaker than they would have been in a smooth medium.

A weak uniform scattering medium will result in high apparent Q values with short and weak attendant coda and a strong uniform scattering medium will result in low apparent Q values with long and energetic coda. The data we observe in the Soviet Union indicates relatively high Q values, which indicates a weak scattering medium, yet the coda are strong, which indicates a strongly scattering medium. A way of resolving this dilemma is to look for other scattering mechanisms which allow for efficient propagation of seismic energy while scattering the coherent arrivals strongly to produce the coda we observe.

We have been investigating such a scattering mechanism which assumes that the structural inhomogeneities are anisotropic, i.e. the scale length of the inhomogeneities is different in the vertical direction than it is in the horizontal direction. The simplest such anisotropic scatterers to model are those which are uniform in the horizontal direction and arbitrarily inhomogeneous in the vertical direction. Of course, this modeling capability has been in existence for some time now, however researchers using laterally homogeneous synthetic seismograms have always used smooth or what we would call "large scale blocky" structural models which will not produce the types of scattering that we would expect in a "random" medium.

The results from a traditional smooth model are shown in figure 10, which displays vertical component synthetic seismograms as a function of source-receiver distance for the structural model given in figures 9a and 9b. The amplitude scales are adjusted by a r^2 factor. The structural model represents the eastern Kazakhstan region and we represent velocity gradients with homogeneous layer approximations. The velocity gradients helped considerably in boosting the relative amplitude of P₁ over what it was without the

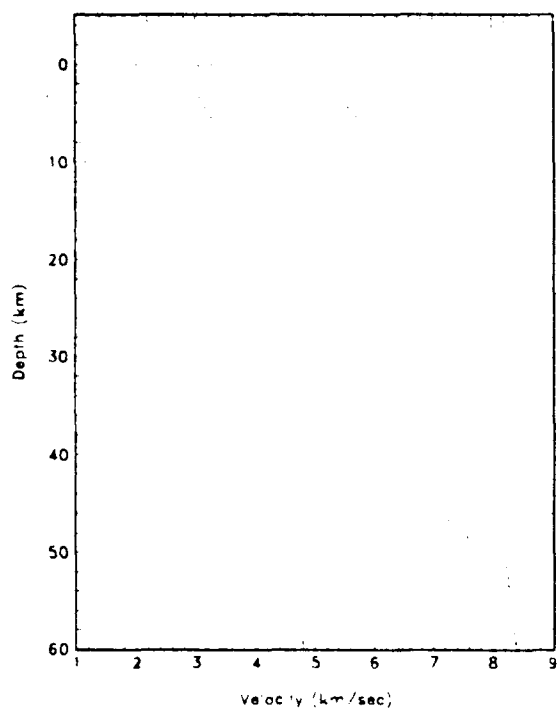


Figure 9a. Base Kazakhstan velocity model

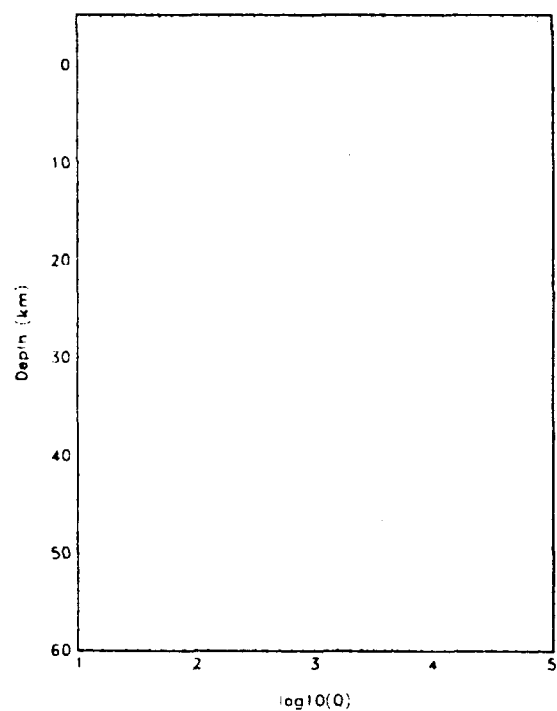


Figure 9b. Base Kazakhstan Q model

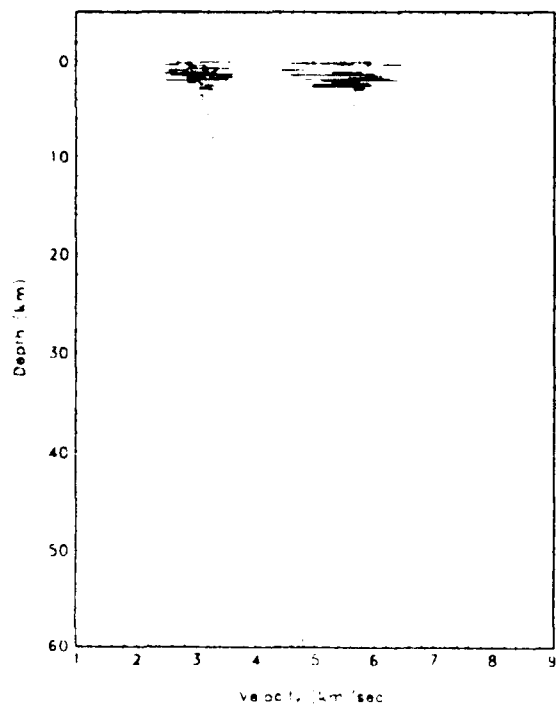


Figure 9c. Randomized velocity model

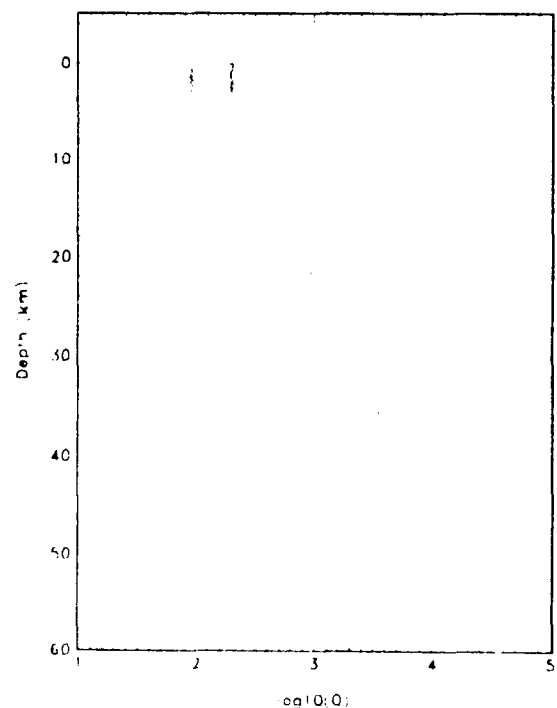


Figure 9d. Randomized Q model

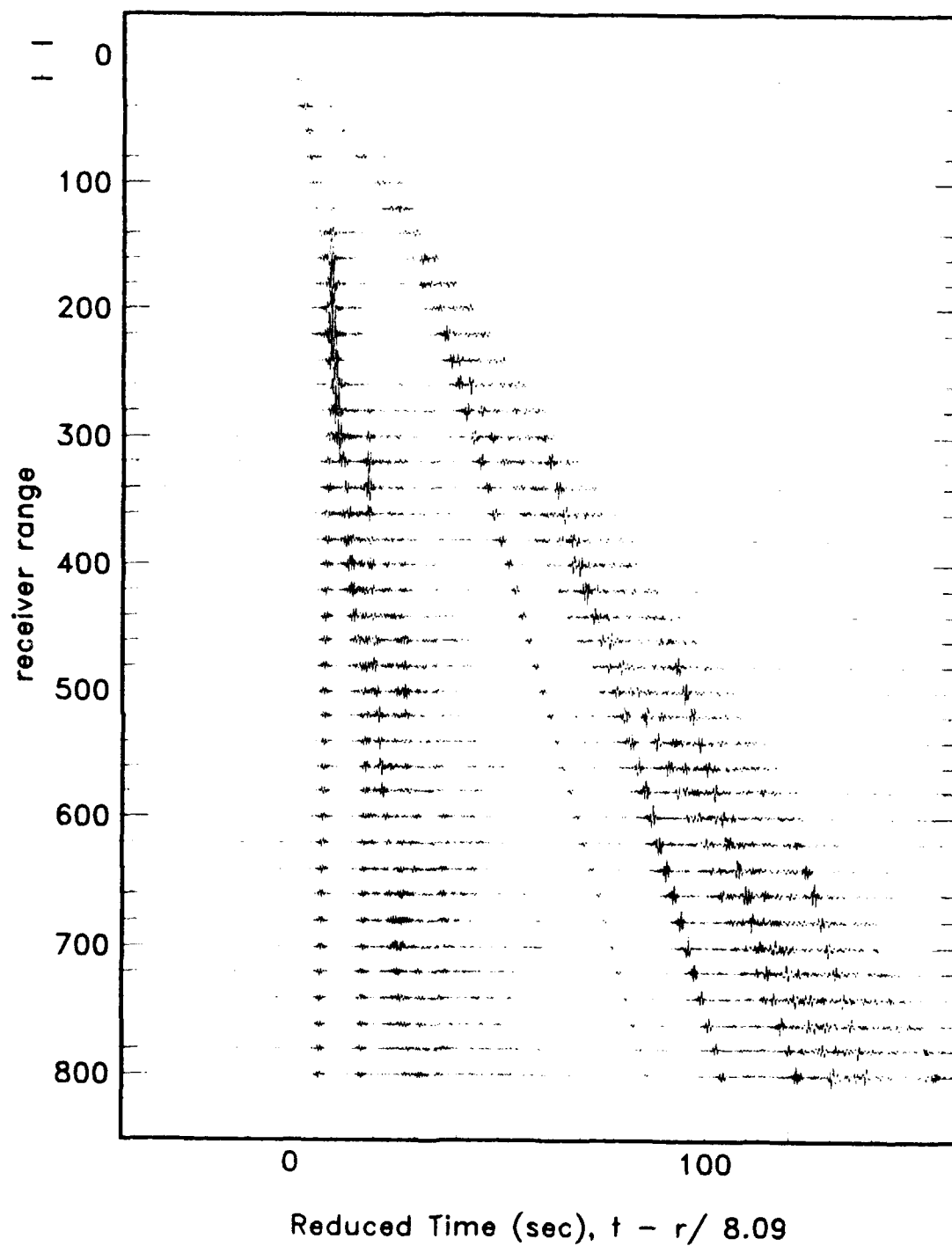


Figure 10. Synthetic vertical components for the base Kazakh model in fig. 9a-9b.

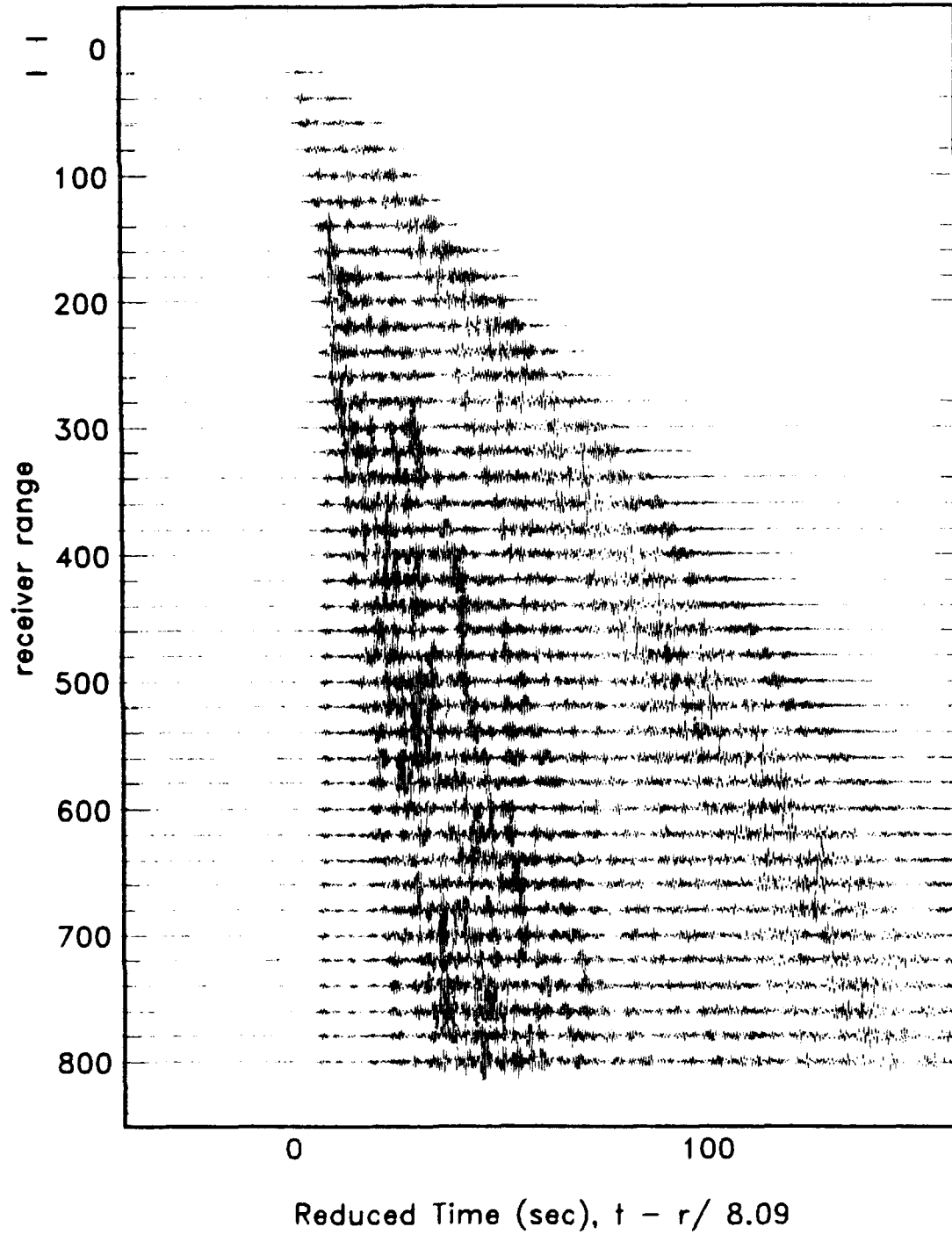


Figure 11. Synthetic vertical components for the randomized model in fig. 9c-9d.

gradients, however the seismograms are simple when compared with the data.

An example of synthetic seismograms produced from a vertically "randomized" structure is shown in figure 11. The amplitude scales are the same as those for figure 10. The structure model is shown in figures 9c-9d and was determined by using the smooth model in figures 9a-9b and applying a random fluctuation with depth dependent layer thickness and variance. We decided to use 100 meter layer thicknesses for the upper 2 km and 1000 meter layer thicknesses elsewhere. We also used high variances near the surface and decreased the variance with depth. Our intent was to crudely match the sort of near surface velocity variances seen in well logging measurements.

A comparison of figure 11 with figure 10 shows many interesting characteristics of anisotropic scattering which are given below.

- Strong and persistent coda are generated throughout the seismograms for the vertically randomized structure. The later arriving phases, P_n , S_n and L_n , although coherent and easy to identify in the smooth structure are incoherent with ambiguous onset times in the vertically randomized structure.
- The seismograms for the vertically randomized structure are much more energetic throughout the duration than those of the smooth structure. Not only has strong coda been generated in the "dead" regions of the seismogram, but the amplitudes of all of the initial arrivals have been preserved as well.

These results are significant in that they show how anisotropic scattering is fundamentally different from isotropic scattering. Instead of attenuating and spreading out the signals as a uniform scattering material would do, a vertically randomized medium focuses the seismic energy while scattering it at the same time. The horizontal laminations introduce numerous low velocity zones with many horizontal layer interfaces that tend to trap the seismic energy similar to the way a fiber optic cable traps light. This energy is free to propagate horizontally, however it is inhibited from propagating vertically and thus energy that would normally propagate away through the bottom of the

structure is kept concentrated in the crust and upper mantle. The introduction of horizontal laminations within a region effectively introduce a *negative* Q effect since they will trap energy within the laminations and thus overcome the normal three dimensional geometric spreading effect. The focusing associated with structural laminations is different from focusing that is normally associated with other three dimensional lenses. Most structural lenses focus seismic energy into small and well defined regions, however structural laminations channel seismic energy into broad horizontal sheets so that the focusing effect can be seen over large distance ranges.

The introduction of vertical randomization into smooth structural models will play an important role in explaining regional seismograms. This gives us an explainable, plausible and implementable method for modeling the features that we see in the data, such as the apparent contradiction of high Q values and strongly scattered coda. We think that this will also strongly effect how Q estimates are made and, ultimately, yield estimations. We can see from these examples that vertical randomization can have very pronounced effects on seismic energy levels that could otherwise be interpreted incorrectly. We were able to pump up the P_n coda arbitrarily by putting large random fluctuations at the depth where, from the differential seismograms, we knew the P_n energy travels. We are currently testing new models in which we have put regions of high lamination at the Moho depth in order to pump up the P_n portion of the seismogram.

In figure 12 we show a comparison of real data with a synthetic seismogram that we computed using the randomized structure given in figures 9c-9d. This shows the vertical component at KKL which was about 250 km from the shot and both the data and the synthetic have been filtered so that the passband of comparison is about 1 to 2 hz. This is one of the best real-synthetic matches of regional data in this frequency range that we have seen and we think that this type of qualitative match is necessary before a formal inversion procedure can be reasonably expected to produce meaningful results.

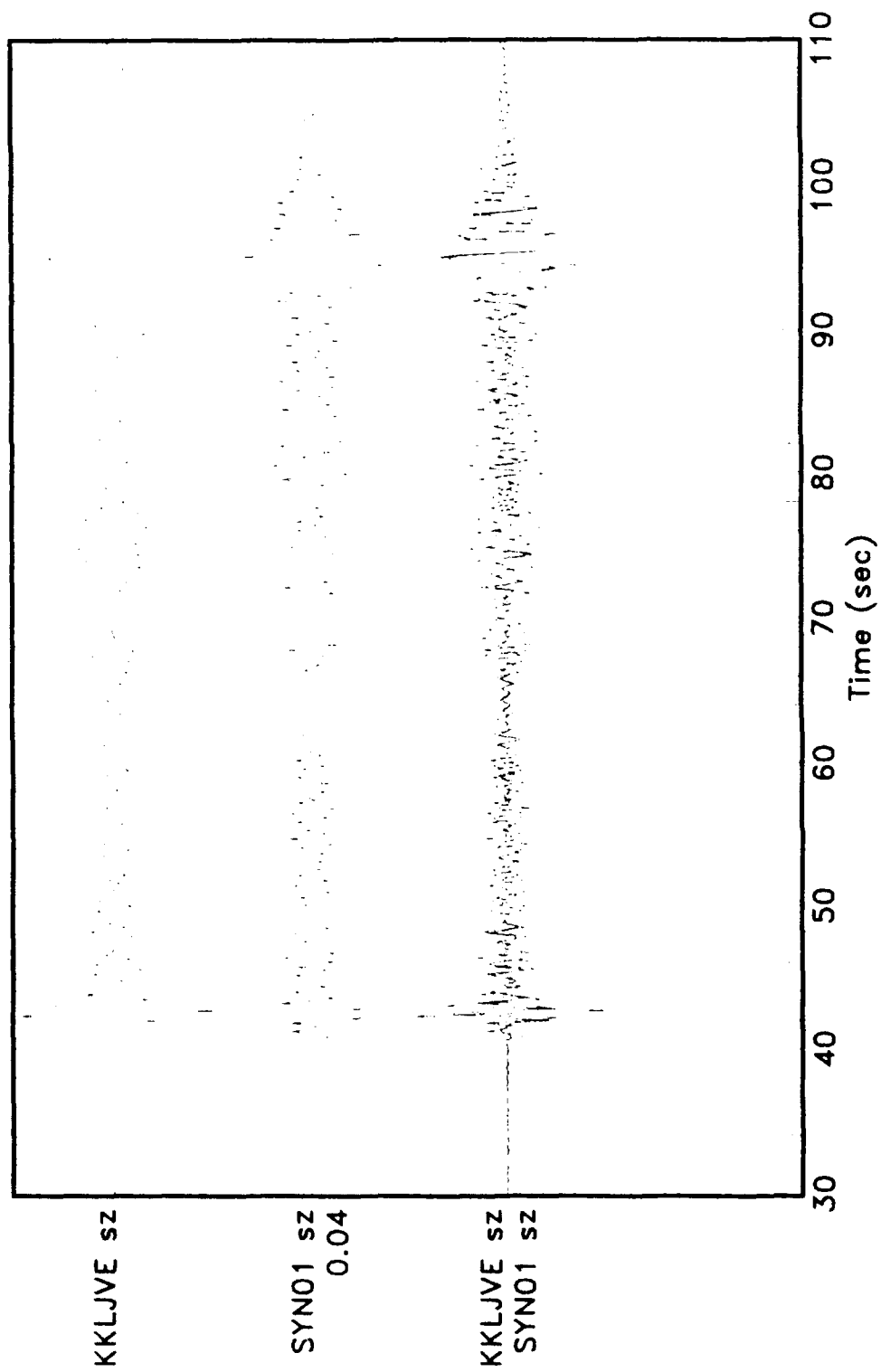


Figure 12. Comparison of real data (KKLJVE) and synthetic (SYN01) for the JVE at station KKL using the structure in fig. 9c-9d.

5. Conclusions

In order to improve our abilities to discriminate low-yield nuclear explosions and to obtain accurate yield estimates, we have undertaken a study to infer detailed source and structure parameters by direct inversion of broad band regional seismic data using laterally homogeneous forward modeling methods. We have identified three key problems which must be solved in order to accomplish our objective: the development of an accurate and efficient algorithm for computing differential seismograms which are necessary for the inversion procedure, the development of better methods for incorporating anelastic attenuation into modal synthesis computations, and the determination of starting solutions that will produce synthetic seismograms which have the same general characteristics that we see in the data.

We have made significant progress in each of these problems. We determined that the normal first order perturbation theory method for computing differential seismograms was inadequate for higher frequencies and phase velocities and we have developed and tested an exact analytic differential seismogram program. We also have developed an exact complex pole based method for computing modal seismograms which avoids the use of first order perturbation theory for incorporating anelastic attenuation. We are in the process of developing an exact first order Q correction along the lines of the exact differential seismogram program which we hope will provide an efficient means for incorporating Q effects.

Our most significant discovery is that anisotropic scattering produces the types of effects that can be seen in the observed data. We consider this to be our most important result to date because it has proven to be difficult to produce synthetic seismograms that match the gross characteristics of broad band regional data. Many researchers attribute this difficulty to complex and indeterminate lateral scattering processes. If they are right, then it is unlikely that we will understand the nature of regional wave propagation and we will be forced to resort almost entirely to empirical methods for doing in-country

yield estimation. We have discovered that an explainable, plausible and implementable method for modeling the features that we see in the data is to use vertically randomized structural models in laterally homogeneous modeling codes.

We think that the idea of horizontal laminations within the earth is very plausible and we have demonstrated that the consequences are significant. We know from well log measurements that the near surface earth structure looks like a stochastic process with depth. We can only speculate about the detailed nature of the structure at depth, however it is unreasonable to rule out the possibility of laminated structures deeper in the earth. A reasonable hypothesis for transition zones, like the Moho, is a region where the material on one side gradually "feathers" into the material on the other side to produce a lamination zone with many thin layers of different material properties. Such a zone could look like a velocity gradient in travel time studies and for longer wave length waves, however at higher frequencies the seismic energy would be efficiently trapped within the laminations.

With the results from our studies to date we feel that we are in a good position to continue our efforts toward the development of full wave regional inversion capabilities. We are continuing our work in this area and we feel confident that we will realize our objectives.

6. Contributing Researchers

The following individuals contributed to the research described in this report.

Dr. Roger Hansen, NORSAR, Kjeller, Norway, currently at the Air Force Technical Applications Center in Cocoa Beach, FL

Dr. Vernon Cormier, University of Connecticut, Storrs, CT

Dr. B. Mandal, Massachusetts Institute of Technology, Cambridge, MA

7. Related Contracts and Publications

A companion contract, "Full Waveform Inversion for Source and Structural Parameters at Regional Distances", F19628-90-K-0050, provided partial support for some of the results presented in this report.

The following publications were produced in part with support from this contract.

Archambeau, C., Harvey, D., and Hansen, R., 1990, Signal propagation characteristics and inferences of elastic-anelastic structure in the USSR, Proceedings of the Twelfth Annual DARPA/GL Seismic Research Symposium, J. Lewkowicz, and J. McPhetres, ed. **GL-TR-90-0212, ADA226635**

Cormier, V. F., Mandal, B., and Harvey, D., 1991, Incorporation of velocity gradients in the synthesis of complete seismograms by the locked mode method, Bulletin of the Seismological Society of America, in press.

Prof. Thomas Ahrens
Seismological Lab, 252-21
Division of Geological & Planetary Sciences
California Institute of Technology
Pasadena, CA 91125

Prof. Keiiti Aki
Center for Earth Sciences
University of Southern California
University Park
Los Angeles, CA 90089-0741

Prof. Shelton Alexander
Geosciences Department
403 Deike Building
The Pennsylvania State University
University Park, PA 16802

Dr. Ralph Alewine, III
DARPA/NMRO
3701 North Fairfax Drive
Arlington, VA 22203-1714

Prof. Charles B. Archambeau
CIRES
University of Colorado
Boulder, CO 80309

Dr. Thomas C. Bache, Jr.
Science Applications Int'l Corp.
10260 Campus Point Drive
San Diego, CA 92121 (2 copies)

Prof. Muawia Barazangi
Institute for the Study of the Continent
Cornell University
Ithaca, NY 14853

Dr. Jeff Barker
Department of Geological Sciences
State University of New York
at Binghamton
Vestal, NY 13901

Dr. Douglas R. Baumgardt
ENSCO, Inc
5400 Port Royal Road
Springfield, VA 22151-2388

Dr. Susan Beck
Department of Geosciences
Building #77
University of Arizona
Tucson, AZ 85721

Dr. T.J. Bennett
S-CUBED
A Division of Maxwell Laboratories
11800 Sunrise Valley Drive, Suite 1450
Reston, VA 22091

Dr. Robert Blandford
AFTAC/IT, Center for Seismic Studies
1330 North 17th Street
Suite 1450
Arlington, VA 22209-2308

Dr. G.A. Bollinger
Department of Geological Sciences
Virginia Polytechnical Institute
21044 Derring Hall
Blacksburg, VA 24061

Dr. Stephen Bratt
Center for Seismic Studies
1300 North 17th Street
Suite 1450
Arlington, VA 22209-2308

Dr. Lawrence Burdick
Woodward-Clyde Consultants
566 El Dorado Street
Pasadena, CA 91109-3245

Dr. Robert Burrige
Schlumberger-Doll Research Center
Old Quarry Road
Ridgefield, CT 06877

Dr. Jerry Carter
Center for Seismic Studies
1300 North 17th Street
Suite 1450
Arlington, VA 22209-2308

Dr. Eric Chael
Division 9241
Sandia Laboratory
Albuquerque, NM 87185

Prof. Vernon F. Cormier
Department of Geology & Geophysics
U-45, Room 207
University of Connecticut
Storrs, CT 06268

Prof. Anton Dainty
Earth Resources Laboratory
Massachusetts Institute of Technology
42 Carleton Street
Cambridge, MA 02142

Prof. Steven Day
Department of Geological Sciences
San Diego State University
San Diego, CA 92182

Dr. Art Frankel
U.S. Geological Survey
922 National Center
Reston, VA 22092

Marvin Denny
U.S. Department of Energy
Office of Arms Control
Washington, DC 20585

Dr. Cliff Frolich
Institute of Geophysics
8701 North Mopac
Austin, TX 78759

Dr. Zoltan Der
ENSCO, Inc.
5400 Port Royal Road
Springfield, VA 22151-2388

Dr. Holly Given
IGPP, A-025
Scripps Institute of Oceanography
University of California, San Diego
La Jolla, CA 92093

Prof. Adam Dziewonski
Hoffman Laboratory, Harvard University
Dept. of Earth Atmos. & Planetary Sciences
20 Oxford Street
Cambridge, MA 02138

Dr. Jeffrey W. Given
SAIC
10260 Campus Point Drive
San Diego, CA 92121

Prof. John Ebel
Department of Geology & Geophysics
Boston College
Chestnut Hill, MA 02167

Dr. Dale Glover
Defense Intelligence Agency
ATTN: ODT-1B
Washington, DC 20301

Eric Fielding
SNEE Hall
INSTOC
Cornell University
Ithaca, NY 14853

Dr. Indra Gupta
Teledyne Geotech
314 Montgomery Street
Alexandria, VA 22314

Dr. Mark D. Fisk
Mission Research Corporation
735 State Street
P.O. Drawer 719
Santa Barbara, CA 93102

Dan N. Hagedorn
Pacific Northwest Laboratories
Battelle Boulevard
Richland, WA 99352

Prof Stanley Flate
Applied Sciences Building
University of California, Santa Cruz
Santa Cruz, CA 95064

Dr. James Hannon
Lawrence Livermore National Laboratory
P.O. Box 808
L-205
Livermore, CA 94550

Dr. John Foley
NER-Geo Sciences
1100 Crown Colony Drive
Quincy, MA 02169

Dr. Roger Hansen
HQ AFTAC/TTR
Patrick AFB, FL 32925-6001

Prof. Donald Forsyth
Department of Geological Sciences
Brown University
Providence, RI 02912

Prof. David G. Harkrider
Seismological Laboratory
Division of Geological & Planetary Sciences
California Institute of Technology
Pasadena, CA 91125

Prof. Danny Harvey
CIRFS
University of Colorado
Boulder, CO 80309

Prof. Donald V. Helmberger
Seismological Laboratory
Division of Geological & Planetary Sciences
California Institute of Technology
Pasadena, CA 91125

Prof. Eugene Herrin
Institute for the Study of Earth and Man
Geophysical Laboratory
Southern Methodist University
Dallas, TX 75275

Prof. Robert B. Herrmann
Department of Earth & Atmospheric Sciences
St. Louis University
St. Louis, MO 63156

Prof. Lane R. Johnson
Seismographic Station
University of California
Berkeley, CA 94720

Prof. Thomas H. Jordan
Department of Earth, Atmospheric &
Planetary Sciences
Massachusetts Institute of Technology
Cambridge, MA 02139

Prof. Alan Kafka
Department of Geology & Geophysics
Boston College
Chestnut Hill, MA 02167

Robert C. Kemerait
ENSCO, Inc.
445 Pineda Court
Melbourne, FL 32940

Dr. Max Koontz
U.S. Dept. of Energy/DP 5
Forrestal Building
1000 Independence Avenue
Washington, DC 20585

Dr. Richard LaCoss
MIT Lincoln Laboratory, M-200B
P.O. Box 73
Lexington, MA 02173-0073

Dr. Fred K. Lamb
University of Illinois at Urbana-Champaign
Department of Physics
1110 West Green Street
Urbana, IL 61801

Prof. Charles A. Langston
Geosciences Department
403 Deike Building
The Pennsylvania State University
University Park, PA 16802

Jim Lawson, Chief Geophysicist
Oklahoma Geological Survey
Oklahoma Geophysical Observatory
P.O. Box 8
Leonard, OK 74043-0008

Prof. Thorne Lay
Institute of Tectonics
Earth Science Board
University of California, Santa Cruz
Santa Cruz, CA 95064

Dr. William Leith
U.S. Geological Survey
Mail Stop 928
Reston, VA 22092

Mr. James F. Lewkowicz
Phillips Laboratory/GPEH
Hanscom AFB, MA 01731-5000(2 copies)

Mr. Alfred Lieberman
ACDA/VI-OA State Department Building
Room 5726
320-21st Street, NW
Washington, DC 20451

Prof. L. Timothy Long
School of Geophysical Sciences
Georgia Institute of Technology
Atlanta, GA 30332

Dr. Robert Masse
Denver Federal Building
Bos 25046, Mail Stop 967
Denver, CO 80225

Dr. Randolph Martin, III
New England Research, Inc.
76 Olcott Drive
White River Junction, VT 05001

Dr. Gary McCartor
Department of Physics
Southern Methodist University
Dallas, TX 75275

Prof. Thomas V. McEvilly
Seismographic Station
University of California
Berkeley, CA 94720

Dr. Art McGarr
U.S. Geological Survey
Mail Stop 977
U.S. Geological Survey
Menlo Park, CA 94025

Dr. Keith L. McLaughlin
S-CUBED
A Division of Maxwell Laboratory
P.O. Box 1620
La Jolla, CA 92038-1620

Stephen Miller & Dr. Alexander Florence
SRI International
333 Ravenswood Avenue
Box AF 116
Menlo Park, CA 94025-3493

Prof. Bernard Minster
IGPP, A-025
Scripps Institute of Oceanography
University of California, San Diego
La Jolla, CA 92093

Prof. Brian J. Mitchell
Department of Earth & Atmospheric Sciences
St. Louis University
St. Louis, MO 63156

Mr. Jack Murphy
S-CUBED
A Division of Maxwell Laboratory
11800 Sunrise Valley Drive, Suite 1212
Reston, VA 22091 (2 Copies)

Dr. Keith K. Nakanishi
Lawrence Livermore National Laboratory
L-025
P.O. Box 808
Livermore, CA 94550

Dr. Carl Newton
Los Alamos National Laboratory
P.O. Box 1663
Mail Stop C335, Group ESS-3
Los Alamos, NM 87545

Dr. Bao Nguyen
HQ AFTAC/TTR
Patrick AFB, FL 32925

Prof. John A. Orcutt
IGPP, A-025
Scripps Institute of Oceanography
University of California, San Diego
La Jolla, CA 92093

Prof. Jeffrey Park
Kline Geology Laboratory
P.O. Box 6666
New Haven, CT 06511-8130

Dr. Howard Patton
Lawrence Livermore National Laboratory
L-025
P.O. Box 808
Livermore, CA 94550

Dr. Frank Pilotte
HQ AFTAC/TT
Patrick AFB, FL 32925-6001

Dr. Jay J. Pulli
Radix Systems, Inc.
2 Taft Court, Suite 203
Rockville, MD 20850

Dr. Robert Reinke
ATIN: FCTVTD
Field Command
Defense Nuclear Agency
Kirtland AFB, NM 87115

Prof. Paul G. Richards
Lamont-Doherty Geological Observatory
of Columbia University
Palisades, NY 10964

Mr. Wilmer Rivers
Teledyne Geotech
314 Montgomery Street
Alexandria, VA 22314

Dr. George Rothe
HQ AFTAC/TTR
Patrick AFB, FL 32925-6001

Dr. Alan S. Ryall, Jr.
DARPA/NMRO
3701 North Fairfax Drive
Arlington, VA 22209-1714

Dr. Richard Sailor
TASC, Inc.
55 Walkers Brook Drive
Reading, MA 01867

Prof. Charles G. Sammis
Center for Earth Sciences
University of Southern California
University Park
Los Angeles, CA 90089-0741

Prof. Christopher H. Scholz
Lamont-Doherty Geological Observatory
of Columbia University
Palisades, CA 10964

Dr. Susan Schwartz
Institute of Tectonics
1156 High Street
Santa Cruz, CA 95064

Secretary of the Air Force
(SAFRD)
Washington, DC 20330

Office of the Secretary of Defense
DDR&E
Washington, DC 20330

Thomas J. Sereno, Jr.
Science Application Int'l Corp.
10260 Campus Point Drive
San Diego, CA 92121

Dr. Michael Shore
Defense Nuclear Agency/SPSS
6801 Telegraph Road
Alexandria, VA 22310

Dr. Matthew Sibol
Virginia Tech
Seismological Observatory
4044 Derring Hall
Blacksburg, VA 24061-0420

Prof. David G. Simpson
IRIS, Inc.
1616 North Fort Myer Drive
Suite 1400
Arlington, VA 22209

Donald L. Springer
Lawrence Livermore National Laboratory
L-025
P.O. Box 808
Livermore, CA 94550

Dr. Jeffrey Stevens
S-CUBED
A Division of Maxwell Laboratory
P.O. Box 1620
La Jolla, CA 92038-1620

Lt. Col. Jim Stobie
ATTN: AFOSR/NL
Bolling AFB
Washington, DC 20332-6448

Prof. Brian Stump
Institute for the Study of Earth & Man
Geophysical Laboratory
Southern Methodist University
Dallas, TX 75275

Prof. Jeremiah Sullivan
University of Illinois at Urbana-Champaign
Department of Physics
1110 West Green Street
Urbana, IL 61801

Prof. L. Sykes
Lamont-Doherty Geological Observatory
of Columbia University
Palisades, NY 10964

Dr. David Taylor
ENSCO, Inc.
445 Pineda Court
Melbourne, FL 32940

Dr. Steven R. Taylor
Los Alamos National Laboratory
P.O. Box 1663
Mail Stop C335
Los Alamos, NM 87545

Prof. Clifford Thurber
University of Wisconsin-Madison
Department of Geology & Geophysics
1215 West Dayton Street
Madison, WS 53706

Prof. M. Nafi Toksoz
Earth Resources Lab
Massachusetts Institute of Technology
42 Carleton Street
Cambridge, MA 02142

Dr. Larry Turnbull
CIA-OSWR/NED
Washington, DC 20505

Dr. Gregory van der Vink
IRIS, Inc.
1616 North Fort Myer Drive
Suite 1440
Arlington, VA 22209

Dr. Karl Veith
EG&G
5211 Auth Road
Suite 240
Suitland, MD 20746

Prof. Terry C. Wallace
Department of Geosciences
Building #77
University of Arizona
Tuscon, AZ 85721

Dr. Thomas Weaver
Los Alamos National Laboratory
P.O. Box 1663
Mail Stop C335
Los Alamos, NM 87545

Dr. William Wortman
Mission Research Corporation
8560 Cinderbed Road
Suite 700
Newington, VA 22122

Prof. Francis T. Wu
Department of Geological Sciences
State University of New York
at Binghamton
Vestal, NY 13901

AFTAC/CA
(STINFO)
Patrick AFB, FL 32925-6001

DARPA/PM
3701 North Fairfax Drive
Arlington, VA 22203-1714

DARPA/RMO/RETRIEVAL
3701 North Fairfax Drive
Arlington, VA 22203-1714

DARPA/RMO/SECURITY OFFICE
3701 North Fairfax Drive
Arlington, VA 2203-1714

HQ DNA
ATTN: Technical Library
Washington, DC 20305

Defense Intelligence Agency
Directorate for Scientific & Technical Intelligence
ATTN: DTIB
Washington, DC 20340-6158

Defense Technical Information Center
Cameron Station
Alexandria, VA 22314 (2 Copies)

TACTEC
Battelle Memorial Institute
505 King Avenue
Columbus, OH 43201 (Final Report)

Phillips Laboratory
ATTN: XPG
Hanscom AFB, MA 01731-5000

Phillips Laboratory
ATTN: GPE
Hanscom AFB, MA 01731-5000

Phillips Laboratory
ATTN: TSML
Hanscom AFB, MA 01731-5000

Phillips Laboratory
ATTN: SUL
Kirtland, NM 87117 (2 copies)

Dr. Michel Bouchon
I.R.I.G.M.-B.P. 68
38402 St. Martin D'Heres
Cedex, FRANCE

Dr. Michel Campillo
Observatoire de Grenoble
I.R.I.G.M.-B.P. 53
38041 Grenoble, FRANCE

Dr. Kin Yip Chun
Geophysics Division
Physics Department
University of Toronto
Ontario, CANADA

Prof. Hans-Peter Harjes
Institute for Geophysics
Ruhr University/Bochum
P.O. Box 102148
4630 Bochum 1, GERMANY

Prof. Eystein Husebye
NTNF/NORSAR
P.O. Box 51
N-2007 Kjeller, NORWAY

David Jepsen
Acting Head, Nuclear Monitoring Section
Bureau of Mineral Resources
Geology and Geophysics
G.P.O. Box 378, Canberra, AUSTRALIA

Ms. Eva Johannisson
Senior Research Officer
National Defense Research Inst.
P.O. Box 27322
S-102 54 Stockholm, SWEDEN

Dr. Peter Marshall
Procurement Executive
Ministry of Defense
Blacknest, Brimpton
Reading FG7-FRS, UNITED KINGDOM

Dr. Bernard Massinon, Dr. Pierre Mechler
Societe Radiomana
27 rue Claude Bernard
75005 Paris, FRANCE (2 Copies)

Dr. Svein Mykkeltveit
NTNF/NORSAR
P.O. Box 51
N-2007 Kjeller, NORWAY (3 Copies)

Prof. Keith Priestley
University of Cambridge
Bullard Labs, Dept. of Earth Sciences
Madingley Rise, Madingley Road
Cambridge CB3 0EZ, ENGLAND

Dr. Jorg Schlittenhardt
Federal Institute for Geosciences & Nat'l Res.
Postfach 510153
D-3000 Hannover 51, GERMANY

Dr. Johannes Schweitzer
Institute of Geophysics
Ruhr University/Bochum
P.O. Box 1102148
4360 Bochum 1, GERMANY